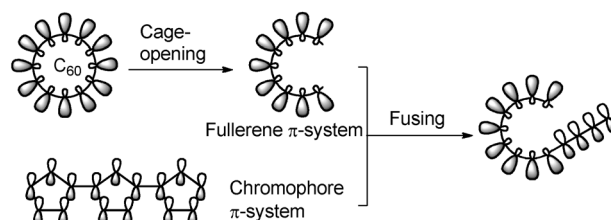


# Pushing Fullerene Absorption into the Near-IR Region by Conjugately Fusing Oligothiophenes\*\*

Zuo Xiao, Gang Ye, Ying Liu, Shan Chen, Qian Peng,\* Qiqun Zuo, and Liming Ding\*

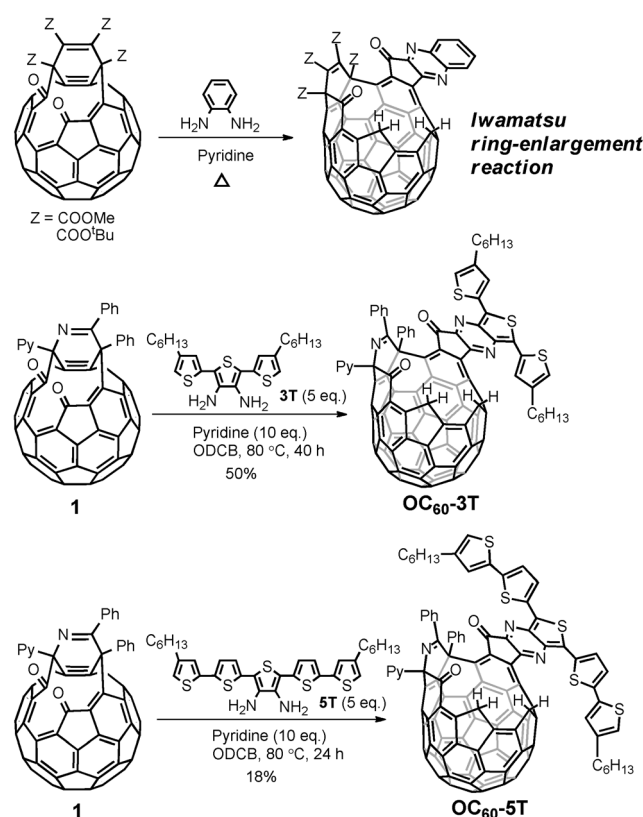
Research in organic electronics and optics is rapidly advancing, and fullerene materials have received more and more attention in this field owing to their unique electronic and photophysical properties.<sup>[1]</sup> Fullerenes are among the best n-type semiconductors for organic solar cells (OSC).<sup>[2]</sup> The power conversion efficiency of conjugated polymer–fullerene solar cells has exceeded 8%.<sup>[3]</sup> Besides, fullerenes have shown their potential in organic thin-film transistors (OTFT) and nonlinear optics (NLO).<sup>[4]</sup> However, the weak visible absorbance and zero near-infrared (NIR) absorbance of fullerene materials are their drawbacks for these applications. For example, in typical polythiophene–fullerene solar cells, the photocurrent contributed from fullerene absorption is only 13% of the total.<sup>[5]</sup> To expand the application of fullerenes in organic electronics and optics, the synthesis of highly light-absorbing fullerene materials is a necessary yet challenging task.<sup>[2a]</sup> Herein, we present the incorporation of an oligothiophene into the fullerene  $\pi$ -system by an open-cage strategy. The absorbance of the new fullerene materials was not only significantly enhanced at the visible region, but also extended to the NIR region. The band gap of the fullerene can be lowered to about 1 eV.

The weak visible absorbance of fullerene originates from its high molecular symmetry, which makes the lowest-energy transitions dipole-forbidden.<sup>[6]</sup> The open-cage strategy proposed here involves cutting the framework of fullerene and fusing an external chromophore into the  $\pi$ -system of fullerene (Scheme 1). Through this modification, the symmetry of fullerene will be reduced, which relaxes the dipole selection rules of low-energy transitions, and the  $\pi$ -system of fullerene will be greatly extended. Therefore, the light-absorbing property of fullerene can be greatly improved.



**Scheme 1.** Open-cage strategy for improving fullerene absorbance.

Iwamatsu et al. reported the synthesis of 20-membered-ring open-cage fullerenes through a novel ring-enlargement reaction between skeleton-modified fullerenes and *ortho*-substituted aromatic diamines.<sup>[7]</sup> Inspired by this work, we designed two *ortho*-diamino-containing oligothiophene chromophores 3T and 5T (Scheme 2). 3T and 5T were prepared through straightforward methods including Stille coupling, reduction, and bromination reactions with 2,5-dibromo-3,4-dinitrothiophene as the starting material (see the Supporting Information). The skeleton-modified fullerene **1** was pre-



**Scheme 2.** Synthesis of OC<sub>60</sub>-3T and OC<sub>60</sub>-5T.

[\*] Dr. Z. Xiao,<sup>[†]</sup> G. Ye,<sup>[†]</sup> Y. Liu, S. Chen, Prof. Dr. L. Ding  
National Center for Nanoscience and Technology  
Beijing 100190 (China)  
E-mail: opv.china@yahoo.com

Dr. Q. Peng  
Institute of Chemistry, Chinese Academy of Sciences  
Beijing 100190 (China)  
E-mail: qpeng@iccas.ac.cn

Q. Zuo  
Jiahong Optoelectronics  
Suzhou 215151 (China)

[†] These authors contributed equally to this work.

[\*\*] This work was supported by the “100 Talents Program” of Chinese Academy of Sciences, National Natural Science Foundation of China (21102028), and Jiahong Optoelectronics.

Supporting information for this article is available on the WWW under <http://dx.doi.org/10.1002/anie.201203981>.

pared according to Murata's open-cage process.<sup>[8]</sup> Treatment of **1** with 3T (or 5T) and pyridine at 80°C afforded the expected orifice-enlarged product, OC<sub>60</sub>-3T, in 50% yield (18% yield for OC<sub>60</sub>-5T). Through this reaction, the  $\pi$ -systems of oligothiophene and fullerene are completely fused to each other by a conjugated pyrazine bridge. OC<sub>60</sub>-3T and OC<sub>60</sub>-5T can be viewed as a new type of fullerene-chromophore dyads, but they are very different from traditional fullerene dyads in which the  $\pi$ -systems of fullerene and the chromophore are separated by a non-conjugated bridge.<sup>[9]</sup> The conjugated bridge helps to realize one integrated conjugation system and may facilitate cross-talking between fullerene and chromophore.<sup>[10]</sup>

OC<sub>60</sub>-3T and OC<sub>60</sub>-5T were thoroughly characterized by spectroscopic methods. A striking feature of the <sup>1</sup>H NMR spectra of these two compounds is that they both show a singlet signal at high field (Figure 1). The signals,

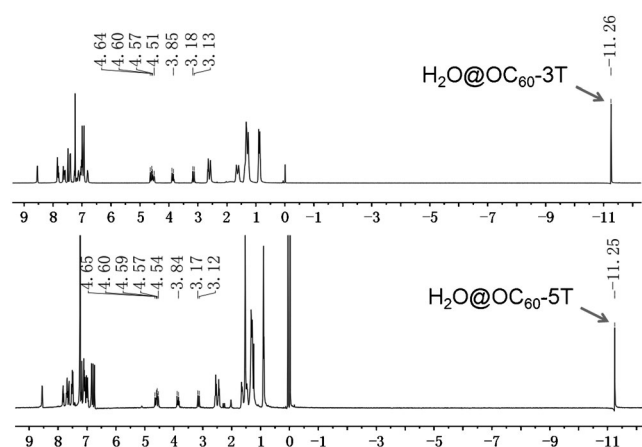


Figure 1. <sup>1</sup>H NMR spectra of OC<sub>60</sub>-3T and OC<sub>60</sub>-5T.

−11.26 ppm for OC<sub>60</sub>-3T and −11.25 ppm for OC<sub>60</sub>-5T, can be assigned to the protons of the H<sub>2</sub>O encapsulated inside fullerene cage. As demonstrated in previous work, water molecules in the solvent enter the fullerene automatically only if the opening on fullerene is large enough for H<sub>2</sub>O to pass through.<sup>[11]</sup> The driving force for this supramolecular phenomenon can be attributed to the strong Lewis acidity of the fullerene cage.<sup>[12]</sup> The large negative chemical shifts of the encapsulated H<sub>2</sub>O are caused by the shielding of fullerene electrons and can in turn provide the solid evidence for the formation of large-orifice open-cage fullerenes.<sup>[13]</sup> Signals at 3.1–4.7 ppm belong to the four characteristic protons of the methylene groups located at the rim of fullerene orifice, which further confirm the structures of OC<sub>60</sub>-3T and OC<sub>60</sub>-5T.<sup>[7,11b]</sup> High-resolution ESI-MS gives the expected molecular ion peaks, 1481.3005 and 1645.2794, for OC<sub>60</sub>-3T and OC<sub>60</sub>-5T, respectively.

The dark color of the dilute solution of OC<sub>60</sub>-3T (dark red) and OC<sub>60</sub>-5T (dark green) indicates the dramatically improved light-absorbing ability of the compounds. The UV/Vis–NIR spectra of OC<sub>60</sub>-3T and OC<sub>60</sub>-5T as well as the references C<sub>60</sub> and C<sub>70</sub> are shown in Figure 2. As expected, OC<sub>60</sub>-3T and OC<sub>60</sub>-5T show greatly improved visible absorp-

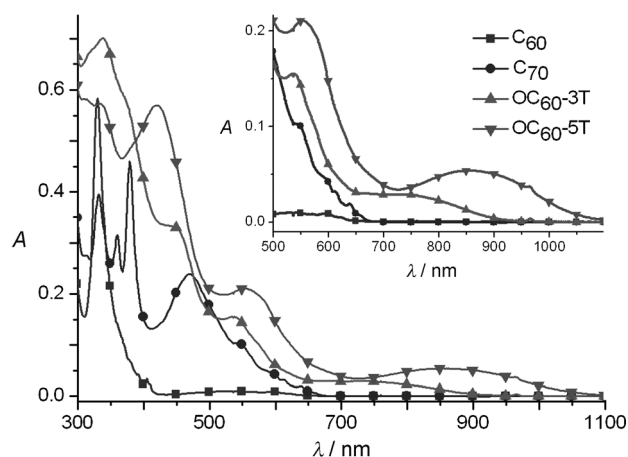


Figure 2. UV/Vis–NIR spectra of C<sub>60</sub>, C<sub>70</sub>, OC<sub>60</sub>-3T, and OC<sub>60</sub>-5T in CHCl<sub>3</sub> (10<sup>−5</sup> M). Inset: enlargement of the spectra at 500–1100 nm.

tion than pristine C<sub>60</sub> and C<sub>70</sub>. Taking the absorbance at 550 nm for example, the molar extinction coefficients for OC<sub>60</sub>-3T and OC<sub>60</sub>-5T are  $1.4 \times 10^4$  and  $2.1 \times 10^4$  L mol<sup>−1</sup> cm<sup>−1</sup>, respectively, which are 15 and 22 times higher than that of C<sub>60</sub>, and 1.4 and 2.1 times higher than that of C<sub>70</sub>. More interestingly, OC<sub>60</sub>-3T and OC<sub>60</sub>-5T exhibit distinct and broad absorption at the NIR region. A step-like absorption covering the range of 700–900 nm is observed for OC<sub>60</sub>-3T. A stronger absorption covering the range of 700–1100 nm with the absorption maximum at 856 nm ( $\epsilon = 0.54 \times 10^4$  L mol<sup>−1</sup> cm<sup>−1</sup>) is observed for OC<sub>60</sub>-5T. The absorption edges of OC<sub>60</sub>-3T and OC<sub>60</sub>-5T are at 920 nm and 1100 nm, respectively. The NIR absorption bands of OC<sub>60</sub>-3T and OC<sub>60</sub>-5T are sensitive to solvent. The bands are slightly blue-shifted in toluene or dioxane compared with that in CHCl<sub>3</sub> (Supporting Information, Figure S12). The solvatochromism of OC<sub>60</sub>-3T and OC<sub>60</sub>-5T indicates that their NIR absorption probably involves with a charge-transfer process.<sup>[14]</sup>

The long-wavelength absorption of OC<sub>60</sub>-3T and OC<sub>60</sub>-5T implies low band gaps of the molecules. We thus investigated the electrochemical properties of the compounds by cyclic voltammetry. OC<sub>60</sub>-3T and OC<sub>60</sub>-5T both show one quasi-reversible oxidation peak and three quasi-reversible reduction peaks. The onset potentials (vs. Fc/Fc<sup>+</sup>) for oxidation and reduction are 0.42 V and −0.88 V for OC<sub>60</sub>-3T and 0.20 V and −0.85 V for OC<sub>60</sub>-5T, respectively. The HOMO and LUMO energy levels of OC<sub>60</sub>-3T and OC<sub>60</sub>-5T were estimated from their onset oxidation and reduction potentials through empirical equations (Table 1).<sup>[15]</sup> The band gaps for OC<sub>60</sub>-3T and OC<sub>60</sub>-5T derived from the difference between LUMO and HOMO are 1.30 eV and 1.05 eV, respectively. To the best of our knowledge, the 1.05 eV band gap for OC<sub>60</sub>-5T is among the lowest band gaps for a fullerene-related  $\pi$ -system.<sup>[16]</sup> Compared to the 1.9 eV band gap for pristine C<sub>60</sub>,<sup>[17]</sup> the much lower band gaps of OC<sub>60</sub>-3T and OC<sub>60</sub>-5T indicate that the open-cage strategy is very effective for tuning the band gaps of fullerenes.

To gain further understanding of the electronic and optical properties of OC<sub>60</sub>-3T and OC<sub>60</sub>-5T, we performed quantum chemical calculations for OC<sub>60</sub>-3T and OC<sub>60</sub>-5T without alkyl

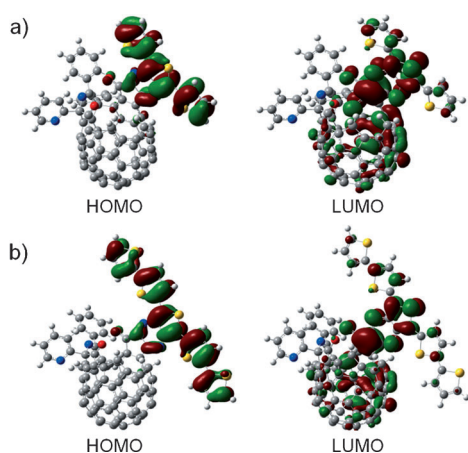
**Table 1:** Optical and electrochemical data.

Compound	$\lambda_{\text{max}}$ [nm]	$E_{\text{ox}}^{\text{on}}$ [V]	$E_{\text{red}}^{\text{on}}$ [V]	HOMO <sup>[a]</sup> [eV]	LUMO <sup>[a]</sup> [eV]	$E_g^{\text{[b]}}$ [V]
OC <sub>60</sub> -3T	338, 543	0.42	−0.88	−5.52 (−5.16) <sup>[c]</sup>	−4.22 (−3.24)	1.30 (1.92)
OC <sub>60</sub> -5T	421, 553, 856	0.20	−0.85	−5.30 (−4.86)	−4.25 (−3.26)	1.05 (1.60)

[a] HOMO and LUMO energy levels were estimated using the following equations:  $\text{HOMO} = -(E_{\text{ox}}^{\text{on}} + 5.1)$  eV,  $\text{LUMO} = -(E_{\text{red}}^{\text{on}} + 5.1)$  eV.

[b]  $E_g = \text{LUMO} - \text{HOMO}$ . [c] Values in the parentheses are theoretical values.

chains. The geometries for OC<sub>60</sub>-3T and OC<sub>60</sub>-5T were optimized at the B3LYP/6-31G\* level. The HOMO and LUMO for the two compounds are shown in Figure 3. It is


**Figure 3.** Frontier orbitals for a) OC<sub>60</sub>-3T and b) OC<sub>60</sub>-5T.

clear that in both cases, the HOMO is localized at the oligothiophene moiety, while the LUMO is mainly localized at the 9*H*-indeno[1,2-*b*]thieno[3,4-*c*]pyrazin-9-one (ITPO) tetracyclic fragment connecting oligothiophene with fullerene, and with some distribution on fullerene sphere. The calculated HOMO and LUMO energy levels are −5.16 and −3.24 eV for OC<sub>60</sub>-3T and −4.86 and −3.26 eV for OC<sub>60</sub>-5T, respectively. Either experimental or theoretical values of the HOMO and LUMO energy levels indicate that from OC<sub>60</sub>-3T to OC<sub>60</sub>-5T, the LUMO drops slightly while the HOMO rises significantly by about 0.3 eV (Table 1). Therefore, the reduction in band gaps of the open-cage fullerenes is mainly caused by the rise of the HOMO, which is located at the oligothiophene moiety. This band-gap tuning process through the open-cage strategy for fullerenes is quite similar to that of the donor–acceptor strategy for developing low-band-gap conjugated copolymers.<sup>[18]</sup>

TD-DFT calculations indicate that the low-energy transition from HOMO to LUMO of OC<sub>60</sub>-3T or OC<sub>60</sub>-5T dominates their NIR absorbance (see the Supporting Information). Considering that the HOMO is at the oligothiophene and the LUMO is mainly at the ITPO fragment, we suggest that the NIR absorption of OC<sub>60</sub>-3T and OC<sub>60</sub>-5T

might originate from intramolecular charge transfer (ICT) from the oligothiophene donor to the ITPO acceptor. To verify this hypothesis, we focus on a model compound N-5T consisting of the same oligothiophene and ITPO moieties as in OC<sub>60</sub>-5T. N-5T was synthesized by condensation of ninhydrin and 5T in 63% yield (Scheme 3). As shown in

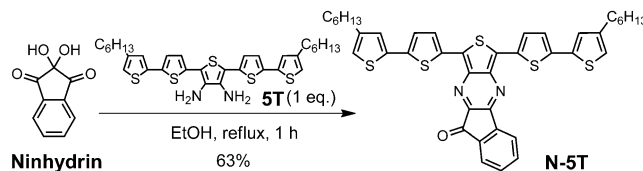
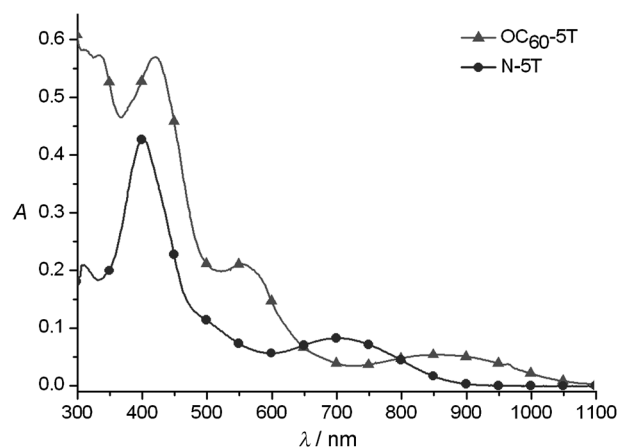

**Scheme 3.** Synthesis of the model compound N-5T.

Figure 4, N-5T exhibits two characteristic absorption bands, one in visible region and the other in NIR region, with absorption maxima at 401 nm ( $\epsilon = 4.3 \times 10^4$  L mol<sup>−1</sup> cm<sup>−1</sup>) and 702 nm ( $\epsilon = 0.83 \times 10^4$  L mol<sup>−1</sup> cm<sup>−1</sup>), respectively. A solvato-


**Figure 4.** UV/Vis–NIR spectra of OC<sub>60</sub>-5T and N-5T in CHCl<sub>3</sub> (10<sup>−5</sup> M).

chromism study indicates that the high-energy band is not sensitive to solvent polarity, while the NIR band is quite sensitive to solvent and shows remarkable blue-shifts (ca. 30 nm) in polar solvents such as dioxane, DMF, and DMSO compared with that in CHCl<sub>3</sub> (Supporting Information, Figure S12). Therefore, the visible absorption could be attributed to the integration of the respective absorption of oligothiophene and ITPO,<sup>[19]</sup> and the NIR absorption might result from ICT.<sup>[14]</sup> Comparison between N-5T and OC<sub>60</sub>-5T absorption spectra indicates that the fullerene  $\pi$ -system has a strong coupling with the  $\pi$ -system of ITPO fragment, which enhances the electron-accepting strength of ITPO and leads to a significant red-shift (152 nm) for ICT band.

In summary, by fusing the  $\pi$ -electron systems of oligothiophene and fullerene through the open-cage strategy, we significantly enhanced the visible absorbance of fullerenes and pushed their absorption into NIR region. This optical property improvement concerns the following factors: 1) symmetry breaking of the fullerene by open-cage reactions allows more low-energy transitions to take place; 2) addi-

Received: May 23, 2012  
Revised: June 27, 2012  
Published online: ■■ ■■, ■■■■

**Keywords:** band gaps · fullerenes · molecular electronics · NIR absorption · quantum chemistry

- [1] F. Langa, J. F. Nierengarten, *Fullerenes: Principles and Applications*, Royal Society of Chemistry, Cambridge, **2007**.
- [2] a) J. L. Delgado, P.-A. Bouit, S. Filippone, M. A. Herranza, N. Martín, *Chem. Commun.* **2010**, 46, 4853; b) Y. He, Y. Li, *Phys. Chem. Chem. Phys.* **2011**, 13, 1970; c) C.-Z. Li, H.-L. Yip, A. K.-Y. Jen, *J. Mater. Chem.* **2012**, 22, 4161.
- [3] Z. He, C. Zhong, X. Huang, W.-Y. Wong, H. Wu, L. Chen, S. Su, Y. Cao, *Adv. Mater.* **2011**, 23, 4636.
- [4] a) J. E. Anthony, A. Facchetti, M. Heeney, S. R. Marder, X. Zhan, *Adv. Mater.* **2010**, 22, 3876; b) C. Waldauf, P. Schilinsky, M. Perisutti, J. Hauch, C. J. Brabec, *Adv. Mater.* **2003**, 15, 2084; c) C. Yang, S. Cho, A. J. Heeger, F. Wudl, *Angew. Chem.* **2009**, 121, 1620; *Angew. Chem. Int. Ed.* **2009**, 48, 1592; d) L. W. Tutt, A. Kost, *Nature* **1992**, 356, 225; e) H. I. Elim, S.-H. Jeon, S. Verma, W. Ji, L.-S. Tan, A. Urbas, L. Y. Chiang, *J. Phys. Chem. B* **2008**, 112, 9561; f) X. Ouyang, H. Zeng, W. Ji, *J. Phys. Chem. B* **2009**, 113, 14565.
- [5] N. C. Nicolaidis, B. S. Routley, J. L. Holdsworth, W. J. Belcher, X. Zhou, P. C. Dastoor, *J. Phys. Chem. C* **2011**, 115, 7801.
- [6] J. W. Arbogast, C. S. Foote, *J. Am. Chem. Soc.* **1991**, 113, 8886.
- [7] S. Iwamatsu, T. Uozaki, K. Kobayashi, S. Re, S. Nagase, S. Murata, *J. Am. Chem. Soc.* **2004**, 126, 2668.
- [8] Y. Murata, M. Murata, K. Komatsu, *Chem. Eur. J.* **2003**, 9, 1600.
- [9] For recent dyad examples, see: a) G. Bottari, G. Torre, D. M. Guldi, T. Torres, *Chem. Rev.* **2010**, 110, 6768; b) V. Garg, G. Kodis, M. Chachisvilis, M. Hambourger, A. L. Moore, T. A. Moore, D. Gust, *J. Am. Chem. Soc.* **2011**, 133, 2944; c) G. de Miguel, M. Wielopolski, D. I. Schuster, M. A. Fazio, O. P. Lee, C. K. Halev, A. L. Ortiz, L. Echegoven, T. Clark, D. M. Guldi, *J. Am. Chem. Soc.* **2010**, 132, 1498.
- [10] L. Gali, D. Yang, Q. Zhang, H. Huang, *Adv. Mater.* **2010**, 22, 1498.
- [11] S. Iwamatsu, S. Murata, *Synlett* **2005**, 2117.
- [12] a) C. Reichardt, T. Welton, *Solvents and Solvent Effects in Organic Chemistry*, Wiley, New York, **2010**; b) A. Marini, A. Muñoz-Losa, A. Biancardi, B. Mennucci, *J. Phys. Chem. B* **2010**, 114, 17128; c) R. Chen, G. Zhao, X. Yang, X. Jiang, J. Liu, H. Tian, Y. Gao, X. Liu, K. Han, M. Sun, L. Sun, *J. Mol. Struct.* **2008**, 876, 102.
- [13] C. M. Cardona, W. Li, A. E. Kaifer, D. Stockdale, G. C. Bazan, *Adv. Mater.* **2011**, 23, 2367.
- [14] a) H. Yang, C. M. Beavers, Z. Wang, A. Jiang, Z. Liu, H. Jin, B. Q. Mercado, M. M. Olmstead, A. L. Balch, *Angew. Chem.* **2010**, 122, 898; *Angew. Chem. Int. Ed.* **2010**, 49, 886; b) T. J. S. Dennis, T. Kai, K. Asato, T. Tomiyama, H. Shinohara, T. Yoshida, Y. Kobayashi, H. Ishiwatari, Y. Miyake, K. Kikuchi, Y. Achiba, *J. Phys. Chem. A* **1999**, 103, 8747; c) C. R. Wang, T. Sugai, T. Kai, T. Tomiyama, H. Shinohara, *Chem. Commun.* **2000**, 557; d) T. Canteenwala, P. A. Padmawar, L. Y. Chiang, *J. Am. Chem. Soc.* **2005**, 127, 26.
- [15] J. H. Weaver, J. L. Martins, T. Komeda, Y. Chen, T. R. Ohno, G. H. Kroll, N. Troullier, R. E. Haufler, R. E. Smalley, *Phys. Rev. Lett.* **1991**, 66, 1741.
- [16] Y.-J. Cheng, S.-H. Yang, C.-S. Hsu, *Chem. Rev.* **2009**, 109, 5868.
- [17] a) M. M. Oliva, T. M. Pappenfus, J. H. Helby, K. M. Schwaderer, J. C. Johnson, K. A. McGee, D. A. S. F. Filho, J. L. Bredas, J. Casado, J. T. L. Navarrete, *Chem. Eur. J.* **2010**, 16, 6866; b) B. D. Pearson, R. A. Mitsch, N. H. Cromwell, *J. Org. Chem.* **1962**, 27, 1674.

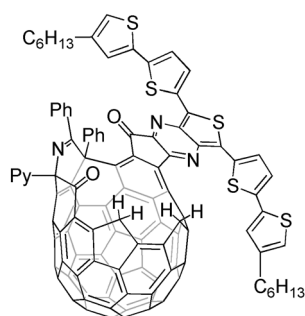
# Communications



## Fullerenes

Z. Xiao, G. Ye, Y. Liu, S. Chen, Q. Peng,\*  
Q. Zuo, L. Ding\* ——— ■■■■—■■■■

Pushing Fullerene Absorption into the  
Near-IR Region by Conjugately Fusing  
Oligothiophenes



**Fusing two in one:** The  $\pi$ -electron systems of fullerene and an oligothiophene were conjugately fused by an open-cage process. This led to novel fullerene–oligothiophene chromophores with significantly enhanced light-absorbing capability, which covers a wide spectral range. The fullerene band gap could be tuned to about 1 eV by a chemical approach.